Helical Macromolecules

Deutsche Ausgabe: DOI: 10.1002/ange.201604071
Internationale Ausgabe: DOI: 10.1002/anie.201604071

Biomimetic Transmembrane Channels with High Stability and Transporting Efficiency from Helically Folded Macromolecules

Chao Lang[+], Wenfang Li[+], Zeyuan Dong, Xin Zhang, Feihu Yang, Bing Yang, Xiaoli Deng, Chenyang Zhang, Jiayun Xu, and Junqiu Liu**

Abstract: *Membrane channels span the cellular lipid bilayers to transport ions and molecules into cells with sophisticated properties including high efficiency and selectivity. It is of particular biological importance in developing biomimetic transmembrane channels with unique functions by means of chemically synthetic strategies. An artificial unimolecular transmembrane channel using pore-containing helical macromolecules is reported. The self-folding, shape-persistent, pore-containing helical macromolecules are able to span the lipid bilayer, and thus result in extraordinary channel stability and high transporting efficiency for protons and cations. The lifetime of this artificial unimolecular channel in the lipid bilayer membrane is impressively long, rivaling those of natural protein channels. Natural channel mimics designed by helically folded polymeric scaffolds will display robust and versatile transport-related properties at single-molecule level.*

Membrane channels span the cellular lipid bilayers to transport ions and molecules into cells with sophisticated properties, including high efficiency and selectivity.[1] Although the functions of biological membrane channels are routinely achieved in nature, it has proved challenging to mimic membrane channels with synthetic systems to replicate the specific functions in terms of affinity, efficiency, stability, and selectivity.[2] Numerous artificial ion channels and nanopores have been recently created by a variety of preparation methods, not only for scientific interest but also for technological applications, such as sensing, separation, and catalysis.[3] However, it is a formidable challenge to create artificial membrane channels possessing the desired features. Natural channels provided the source of inspiration, which allows their structures and functions to be mimicked and even improved upon. As a type of highly sophisticated example, the biological membrane-spanning protein pores provide precious information in both structural complexity and functional diversity. A surprisingly simple channel is the naturally occurring peptide gramicidin A (gA), which consists of alternating D- and L-amino acids to form a helix dimer with 2.6 nm length and approximate 0.40 nm in diameter.[4] The fact that natural helices were selectively evolved into biological membrane channels will inspire the design of artificial helical macromolecules capable of achieving a predictable structure with specific transport properties. The traditional scaffolds of polypeptides and polymers are generally too flexible to generate predictable and definite pore structures. To overcome the inherent shortcomings, synthetic rigid polymers that can fold into stable helical structures in solution are promising to be designed as pore-containing scaffolds for the construction of artificial transmembrane channels.

In the biopolymers, the folding of polymeric chains resulted in their well-defined structures, such as the DNA duplex or the highly ordered structures of proteins, and hence determined their biological functions. Recently, biomimetic design of helical structures has been developed promptly, which gave rise to the generation of functional diversity including chirality separation, optoelectronic, sensors, catalysis, and molecular motors.[5] With few exceptions,[6,7] however, the function of membrane-spanning transport based on helically single-molecular pore structures has not yet been fully realized. Therefore, it is of particular biological importance to create a channel mimic by using helically polymeric scaffolds with desirable pore structures, and thus to exploit the transport-related functions via a channel model system.

We previously reported our design strategy on a type of pore-containing helical macromolecules, and fully characterized their structures.[8] In a clear single-molecular imaging from scanning tunneling microscopy, the structural parameters of the helical macromolecules were clearly revealed. The excellent pore size (ca. 0.55 nm) might make this kind of macromolecules available to ions transport across the lipid bilayers. Herein, we successfully achieved the synthesis of pore-containing helical macromolecules with ideal length of 3.3 nm according to the previous method with side chain substituent modification. The transport-related functions of this kind of helical macromolecules will be uncovered in an artificial channel system (Figure 1).

To design a functional ion channel with rigid helical macromolecules, a prerequisite is to make helically molecular backbones long enough for spanning the lipid bilayer. It is synthetically difficult to obtain large rigid helical macromolecule so far,[9] owing to the fact that steric hindrance caused by the helical matrix constrains the high-molecular-weight polymerization. Additionally, the solubility issue will also be an interference factor to the synthesis of rigid nanometer-scaled helical macromolecules. To overcome these issues, an alternative pre-polymerization method was

[*] Dr. C. Lang,[+] Dr. W. F. Li,[+] Prof. Z. Y. Dong, Dr. X. Zhang, F. H. Yang, Prof. B. Yang, X. L. Deng, C. Y. Zhang, J. Y. Xu, Prof. J. Q. Liu
State Key Laboratory of Supramolecular Structure and Materials, College of Chemistry, Jilin University
2699 Qianjin Street, Changchun 130012 (P.R. China)
E-mail: zdong@jlu.edu.cn
junqiuliu@jlu.edu.cn

[+] These authors contributed equally to this work.

Supporting information for this article can be found under: http://dx.doi.org/10.1002/anie.201604071.

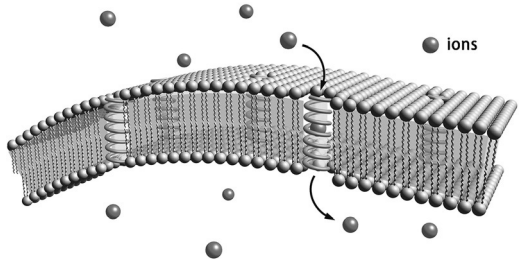

Figure 1. Representation of the membrane-spanning ion transport of pore-containing helical macromolecules in a lipid bilayer system.

adopted, and the solubilizing side chains were introduced into the polymeric backbones. The liner hydrazide macromolecules (Figure 2) were readily synthesized as precursors to

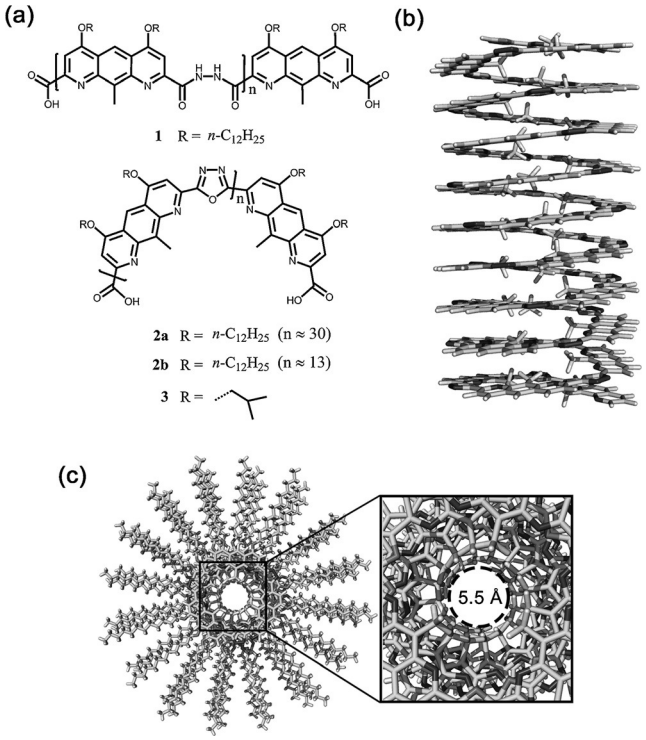

Figure 2. a) Macromolecular structures (**1**–**3**) used in this study and b), c) conformational model of helical macromolecule **2a** illustrated with the COMPASS force field. The pore size is estimated to be about 0.55 nm.

achieve high polymerization degree, and then the high molecular weight helical macromolecules were produced via a cyclization step. By GPC, the number average molecular weight and PDI of macromolecule **2a** were determined to be 18700 and 1.21, respectively. According to the helical pitch of 0.36 nm and 3.2 units per turn in this kind of helical macromolecules, the average length of **2a** is calculated to be 3.3 nm, which is longer than the gA dimer. A shorter polymer **2b** with molecular weight of 7900 (1.4 nm in length) and PDI of 1.09 was also synthesized to be used for comparison.

To construct a transmembrane channel model, we wondered if the helical macromolecules were able to properly plug into the lipid bilayer. We utilized fluorescence microscope imaging to explore the interactions between helical macromolecules and giant unilamellar vesicles (GUVs). As shown in Figures 3a,b, no obvious difference was found

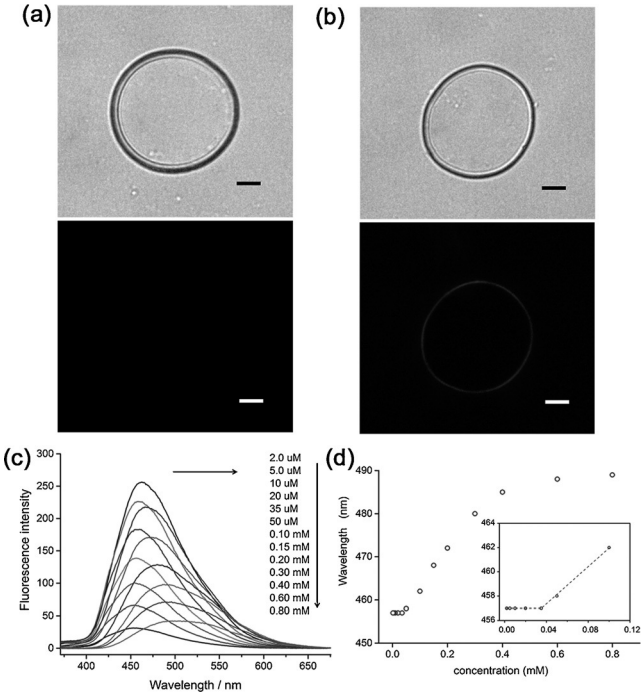

Figure 3. Fluorescence imaging and titration of the helix channel. GUV imaged in bright field and fluorescence mode (excitation: 365 nm). a) Images of pure GUV; b) Images of **2a**·GUV, scale bar = 10 μm. c) Fluorescence titration of **2a** (excitation: 365 nm). d) Quantified analysis of the relationship between maximum emission wavelength and the molar concentration of **2a**.

between the bright field images of formed GUV with or without **2a**. In the fluorescence mode, however, no signal was detected in the pure phospholipid vesicles while the complexation mixture of **2a** and GUV (**2a**·GUV) exhibited significant fluorescence around the wall of GUVs. This result demonstrated that helical macromolecule **2a** was able to insert into the lipid bilayers while membrane structure remained intact.

Concentration-dependent fluorescence titration was carried out to distinguish between a single helix and double helix of **2a** for performing transmembrane transport function, since this type of helical macromolecules are inclined to self-assemble into a double helix by the dimerization of the single helix.[8] As the concentration of **2a** increased, the emission wavelength changed from 457 nm to 489 nm corresponding to the single helix interconverting to double helix (Figures 3c,d). The emission wavelength at 457 nm matches the blue fluorescence observed within **2a**·GUV, indicating that **2a** acts as a single helix form inside the lipid membrane. The result is within expectation since the starting concentration on transformation was about 40 μM (Figure 3d, inset), which is far beyond the concentration (below 8 μM) used in the channel test experiments. Moreover, the length of single helix of **2a** matched well with the thickness of hydrophobic

area of lipid membrane, whereas double helix is two-fold longer than single helix. These results strongly supported that **2a** exists as a single-stranded helix inside the lipid membrane.

The proton (H^+) transport activity of helical macromolecules was evaluated by means of the HPTS assay.[10] As shown in Figure 4a, **2a** and **2b** can transport H^+ at very low channel loading, while the transport activities of **1** and **3** were almost undetected even at the high concentration. The absence of transport ability of **1** strongly suggested that the pore structure of the helix should be critical and indispensable for the ion transport capability of **2**. Furthermore, the poor activity of **3** is mainly ascribed to the weak solubility and membrane insertion compatibility. When the isobutyl side chains of **3** were substituted by the dodecyl groups, the resultant helical macromolecule **2** displayed effective ion channel properties. 5(6)-carboxyfluorescein (CF) experiments were also performed with **2** to rule out non-selective leakage caused by membrane defects (Supporting Information, Figure S2).

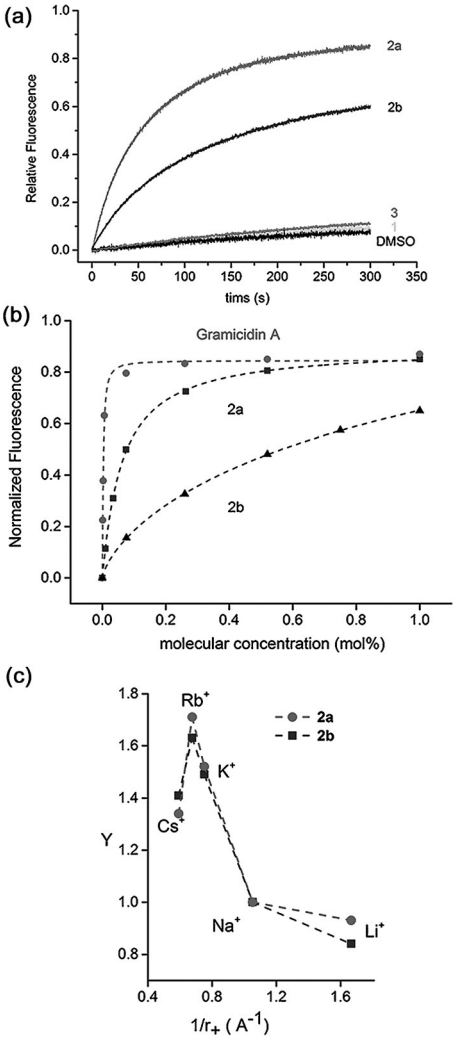

Figure 4. Ion transport assessed with large unilamellar vesicles. a) Normalized H^+ transport activity of **2a** (0.6 mol%), **2b** (0.6 mol%), **3** (5.0 mol%), and **1** (5.0 mol%). b) Hill analysis of the dose-response profile of H^+ transport for **2a**, **2b** and gA. c) Cation selectivity of **2a** and **2b** presented as normalized activity Y (normalized to Na^+) on the reciprocal cation radius.

To investigate the transport property of the helices quantitatively, Hill analysis was performed. The analyses gave EC_{50} values of 0.08 mol%, 0.56 mol%, and 0.001 mol% for **2a**, **2b**, and gA, respectively. This result proved that **2** are able to act as highly effective transmembrane channels, compared to the natural channel gA (Figure 4b). The significant activity difference between both **2a** and **2b** also implied that the length of helix is a critical factor that affects the transporting efficiency. Considering the length match of **2a** (3.3 nm) or **2b** (1.4 nm) with the thickness of the hydrophobic area of lipid bilayer (ca. 3.5 nm), it was proposed that the whole macromolecule **2a** will function as a unimolecular channel, while the short **2b** would stack into a supramolecular channel via π–π interactions, inserting into the lipid bilayer.[7,8] The Hill coefficient *n* is related to the number of monomers involved in the active transport system, which is determined to be 1.7 for gA compared with 1 for **2a** and 0.6 for **2b**. The small Hill coefficients of **2a** and **2b** implied that the helical macromolecule channel systems are thermodynamically stable.[11] In particular, the Hill coefficient is 1; in combination with the above fluorescence-related experimental evidence, it is strongly demonstrated that the conducting form of **2a** is a unimolecular channel in the lipid bilayer membrane.

The highly efficient H^+ transport properties of **2a** and **2b** inspired us to further explore their cation transport abilities. It was found that the cation transport activities of **2a** and **2b** were in the same order $Rb^+ > K^+ > Cs^+ > Na^+ > Li^+$ (Figure 4c; Supporting Information, Figure S3), following the Eisenman sequence III.[12] The identical ion selectivity of the unimolecular channel **2a** and the self-assembled channel **2b** is consistent with the rational design in which ions were conducted through the interior of the helix, namely, the lumen of the channel structure. Although the cation selectivity of channel mimic possibly needed further investigation in future (molecular simulation data in the Supporting Information, Figure S11), the pore transport was in action in the helical macromolecules. In contrast, the selectivity for anions was found to be negligible in an anion titration experiment (Supporting Information, Figure S4), indicating in that channel **2**, cations are preferred.

To illuminate the nature of ion transport of helical macromolecule channels, the single-channel electrophysiology of **2** was investigated with planar lipid bilayers. As seen in Figure 5, **2a** and **2b** both displayed very stable square signals, providing ultimate evidence of **2** forming ion channel in the lipid bilayer. The steady long-lasting single-channel current is particularly interesting because of the revealed potential in future utilization of the system for single-molecular sensing, like stochastic DNA sequencing or the detection of chemical reactions. As shown, gA has a channel lifetime less than two seconds under the identical conditions, which is much shorter than **2** (Figure 5c; Supporting Information, Figure S8). The channel dwell time of **2a**, ranging from tens of seconds to several minutes, is impressively long, which goes beyond most synthetic ion channel systems reported previously.[13] The

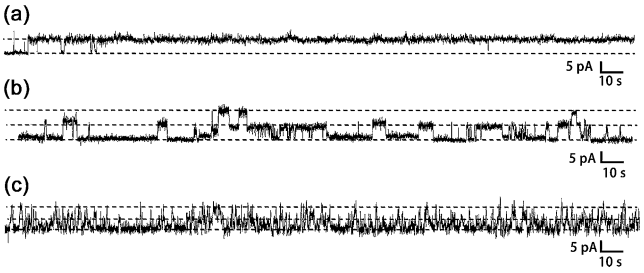

Figure 5. Planar lipid bilayer experiments of the helix channel. Electrophysiology channel recordings of a) **2a**, b) **2b**, and c) Gramicidin A in a symmetrical 0.5 M KCl solution at +150 mV.

remarkable stability of **2a** is ascribed to the robust pore framework for steady ion transport in this well-matched transmembrane model system.

Another notable observation is that the channel lifetime of **2b** is substantially shorter than **2a**. The relatively frequent gating behavior for **2b** was caused by the dynamic feature of self-assembled supramolecular channel (Figure 5b). The result is also reminiscent of the longer channel lifetime of covalently linked gA dimer than its natural form.[4] Compared to the short helix **2b**, the long helical macromolecule **2a** itself can form a unimolecular ionic channel, thus possessing better stability and longer lifetime.

As one of the key parameters of ion channels, the conductance was calculated using the obtained *I–V* plot (Figure 6). We found that the conductance is 61 pS and 59 pS for **2a** and **2b**, respectively, both are very similar but larger than 39 pS for gA under identical conditions. This suggested that in the conducting pathway the pore structure rather than the helix molecule size displayed major contribution on the channel conductance. From the Hille equation,[14] the pore size of **2a** was evaluated to be 0.48 nm, which is slightly smaller than the value from the calculated model (0.55 nm). The *I–V* plot was also measured in asymmetrical solutions to test K^+/Cl^- permeation ratio of **2a** (Figure 6b), which was calculated to be 5.7 according to the Goldman–Hodgkins–Katz analysis.[12]

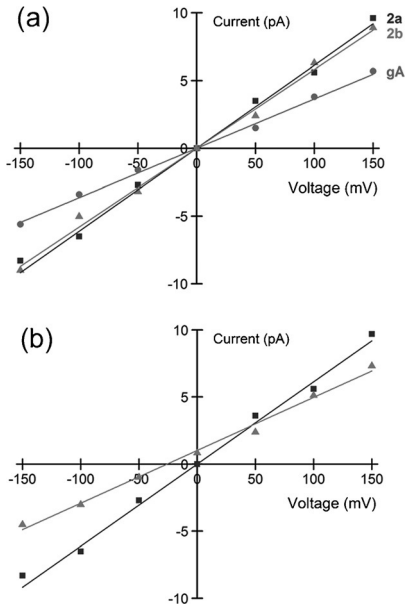

Figure 6. *I–V* plot of a) **2a**, **2b**, and gA determined in a symmetrical 0.5 M KCl solution and b) **2a** determined in asymmetrical solutions. ■ 0.5 M KCl in *cis* and *trans* chamber; ▲ 0.1 M KCl in *cis* chamber, 0.5 M KCl in *trans* chamber.

In conclusion, we successfully realized biomimetic transmembrane transport by using pore-containing helical macromolecules as unimolecular channels. This type of helical macromolecule was designed and synthesized by means of pre-polymerization method, which is very effective to produce a long and stable pore-containing helical polymer. The helical macromolecule channels displayed very interesting transport-related properties, and in particular extraordinary channel stability and high transport efficiency. Significantly, the lifetime of artificial helical macromolecule channel in the lipid bilayer membrane is quite long, rivaling those of natural transmembrane protein channels. Helical macromolecule channels displayed highly efficient transporting abilities, which show great potential in the fabrications of artificial transmembrane channels and nanopore materials with a large amount of synthetically accessible and modifiable helical polymers. The success of the unimolecular channel mimic by using helically polymeric scaffolds will also be helpful to open the structure–function relationships of naturally occurring channels.

Acknowledgements

This work was supported by the Natural Science Foundation of China (No: 21274051, 21574054, 21234004, 21420102007, 21574056, 91527302), and the Chang Jiang Scholars Program of China.

Keywords: cation transport · helical folding · helical macromolecules · pore structure · transmembrane channels

How to cite: *Angew. Chem. Int. Ed.* **2016**, *55*, 9723–9727
Angew. Chem. **2016**, *128*, 9875–9879

[1] B. Hille, *Ionic Channels of Excitable Membranes*, *3rd ed.*, Sinauer Associates, Sunderland, **2001**.

[2] a) S. Matile, A. V. Jentzsch, J. Montenegro, A. Fin, *Chem. Soc. Rev.* **2011**, *40*, 2453–2474; b) T. M. Fyles, *Acc. Chem. Res.* **2013**, *46*, 2847–2855; c) G. W. Gokel, S. Negin, *Acc. Chem. Res.* **2013**, 46, 2824–2833; d) J. Montenegro, M. R. Ghadiri, J. R. Granja, *Acc. Chem. Res.* **2013**, *46*, 2955–2965; e) M. J. Pregel, L. Jullien, J. M. Lehn, *Angew. Chem. Int. Ed. Engl.* **1992**, *31*, 1637–1640; *Angew. Chem.* **1992**, *104*, 1695–1697; f) X. Zhou, G. Liu, K. Yamato, Y. Shen, R. Cheng, X. Wei, W. Bai, Y. Gao, H. Li, Y. Liu, F. Liu, D. M. Czajkowsky, J. Wang, M. J. Dabney, Z. Cai, J. Hu, F. V. Bright, L. He, X. C. Zeng, Z. Shao, B. Gong, *Nat. Commun.* **2012**, *3*, 949; g) W. Si, P. Xin, Z.-T. Li, J.-L. Hou, *Acc. Chem. Res.* **2015**, *48*, 1612–1619.

[3] a) S. Litvinchuk, H. Tanaka, T. Miyatake, D. Pasini, T. Tanaka, G. Bollot, J. Mareda, S. Matile, *Nat. Mater.* **2007**, *6*, 576–580; b) D. L. Gin, R. D. Noble, *Science* **2011**, *332*, 674–676; c) M. Mayer, J. Yang, *Acc. Chem. Res.* **2013**, *46*, 2998–3008; d) M.

Langecker, V. Arnaut, T. G. Martin, J. List, S. Renner, M. Mayer, H. Dietz, F. C. Simmel, *Science* **2012**, *338*, 932 – 936; e) A. G. Cioffi, J. Hou, A. S. Grillo, K. A. Diaz, M. D. Burke, *J. Am. Chem. Soc.* **2015**, *137*, 10096 – 10099.

[4] a) D. W. Urry, M. C. Goodall, J. D. Glickson, D. F. Mayers, *Proc. Natl. Acad. Sci. USA* **1971**, *68*, 1907 – 1911; b) C. J. Stankovic, S. H. Heinemann, J. M. Delfino, D. J. Sigworth, S. L. Schreiber, *Science* **1989**, *244*, 813 – 817; c) R. R. Ketchem, W. Hu, T. A. Cross, *Science* **1993**, *261*, 1457 – 1460; d) D. W. Urry, *Proc. Natl. Acad. Sci. USA* **1971**, *68*, 672 – 676.

[5] a) E. Yashima, K. Maeda, H. Iida, Y. Furusho, K. Nagai, *Chem. Rev.* **2009**, *109*, 6102 – 6211; b) V. Berl, I. Huc, R. G. Khoury, M. J. Krische, J. M. Lehn, *Nature* **2000**, *407*, 720 – 723; c) D. Pijper, B. L. Feringa, *Angew. Chem. Int. Ed.* **2007**, *46*, 3693 – 3696; *Angew. Chem.* **2007**, *119*, 3767 – 3770; d) K. Shimomura, T. Ikai, S. Kanoh, E. Yashima, K. Maeda, *Nat. Chem.* **2014**, *6*, 429 – 434; e) H. Onouchi, T. Miyagawa, K. Morino, E. Yashima, *Angew. Chem. Int. Ed.* **2006**, *45*, 2381 – 2384; *Angew. Chem.* **2006**, *118*, 2441 – 2444; f) M. Reggelin, S. Doerr, M. Klussmann, M. Schultz, M. Holbach, *Proc. Natl. Acad. Sci. USA* **2004**, *101*, 5461 – 5466; g) Y. Huo, H. Zeng, *Acc. Chem. Res.* **2016**, DOI: 10.1021/acs.accounts.6b00051.

[6] P. Xin, P. Zhu, P. Su, J.-L. Hou, Z.-T. Li, *J. Am. Chem. Soc.* **2014**, *136*, 13078 – 13081.

[7] H. Zhao, S. Sheng, Y. Hong, H. Zeng, *J. Am. Chem. Soc.* **2014**, *136*, 14270 – 14276.

[8] J. Zhu, Z. Dong, S. Lei, L. Cao, B. Yang, W. Li, Y. Zhang, J. Liu, J. Shen, *Angew. Chem. Int. Ed.* **2015**, *54*, 3097 – 3101; *Angew. Chem.* **2015**, *127*, 3140 – 3144.

[9] a) J. J. van Gorp, J. A. J. M. Vekemansa, E. W. Meijer, *Chem. Commun.* **2004**, 60 – 61; b) Y. X. Lu, Z. M. Shi, Z. T. Li, Z. Guan, *Chem. Commun.* **2010**, *46*, 9019 – 9021.

[10] N. R. Clement, J. M. Gould, *Biochemistry* **1981**, *20*, 1534 – 1538.

[11] S. Matile, N. Sakai, In Analytical Methods in Supramolecular Chemistry; Wiley-VCH: Weinheim, **2012**, **p.** 711.

[12] G. Eisenman, R. Horn, *J. Membr. Biol.* **1983**, *76*, 197 – 225.

[13] J. K. W. Chui, T. M. Fyles, *Chem. Soc. Rev.* **2012**, *41*, 148 – 175.

[14] O. S. Smart, J. Breed, G. R. Smith, M. S. P. Sansom, *Biophys. J.* **1997**, *72*, 1109 – 1126.

Received: April 27, 2016
Published online: June 29, 2016

